Synthesis and Structure of New (Polyphosphane)ruthenium Complexes with the Hemilabile Ligand 2-(Diphenylphosphanyl)-1-methyl-1*H*-imidazole − An Unexpected Rearrangement of $[RuCl_2(PN)(PPh_3)_2]$

Gustavo Espino,[a] Félix A. Jalón,[b] Miguel Maestro,[c] Blanca R. Manzano,*[b] Mercedes Pérez-Manrique,[a] and Ana C. Bacigalupe[a]

Keywords: Ruthenium / Hemilabile ligands / Hydride ligands / Phosphanes / N,P ligands

Several Ru^{II} complexes containing the potentially bidentate ligand 2-(diphenylphosphanyl)-1-methyl-1*H*-imidazole [PPh_2MeIm (PN)] have been synthesised and characterised. Reaction of the ligand with $[RuCl_2(PPh_3)_3]$ in different molar ratios led to the formation of the complexes *trans*,*mer*-$[RuCl_2(PPh_3)_2(\kappa^2\text{-}P,N\text{–}PPh_2MeIm)]$ (**1**), *fac*-$[RuCl(PPh_3)(\kappa^2\text{-}P,N\text{-}PPh_2MeIm)_2]Cl$ (**2a**), *mer*-$[RuCl(PPh_3)(\kappa^2\text{-}P,N\text{-}PPh_2MeIm)_2]Cl$ (**2b**), *fac*-$[RuCl(\kappa^1\text{-}P\text{-}PPh_2MeIm)(\kappa^2\text{-}P,N\text{-}PPh_2MeIm)_2]Cl$ (**3a**), and *mer*-$[RuCl(\kappa^1\text{-}P\text{-}PPh_2MeIm)(\kappa^2\text{-}PN\text{-}PPh_2MeIm)_2]Cl$ (**3b**). Complex **1** evolves in solution to **2a**, **2b** and the dinuclear species $[(PPh_3)(\kappa^1\text{-}P\text{-}PPh_2MeIm)ClRu(\mu\text{-}Cl)_2Ru(PPh_3)(\kappa^1\text{-}P\text{-}PPh_2MeIm)Cl]$ (**4a**), $[(PPh_3)ClRu(\mu\text{-}Cl)_2(\mu^2\text{-}P,N\text{-}PPh_2MeIm)_2Ru(PPh_3)Cl]$ (**4b**), and $[(PPh_3)(\kappa^2\text{-}P,N\text{-}PPh_2MeIm)ClRu(\mu\text{-}Cl)_2Ru(PPh_3)(\kappa^2\text{-}P,N\text{-}PPh_2MeIm)Cl]$ (**4c**). It is proposed that the formation of the dinuclear derivatives involves an Ru–N bond-breaking step that demonstrates the hemilabile behaviour of the ligand. When 2 equiv. of the PN ligand were added to $[RuCl_2(cod)(bpzm)]$ [cod = 1,5-cyclooctadiene, bpzm = bis(pyrazol-1-yl)methane], the complex *cis*-*P*-$[RuCl_2(\kappa^1\text{-}PPh_2MeIm)(\kappa^2\text{-}PPh_2MeIm)]$ (**5**) was formed as the only product. The derivatives $[Ru(\kappa^2\text{-}PPh_2MeIm)_3]X_2$ [(X = PF_6 (**6**), BF_4 (**7**)] were obtained upon treatment of $[RuCl_2(arene)]_2$ (arene = *p*-cymene, benzene) with 2 equiv. of the corresponding silver salts and the PN ligand. Both the *fac* (**6a**, **7a**) and *mer* (**6b**, **7b**) forms were obtained. Two new hydride complexes were also synthesised: *mer*-$[RuHClL_2(\kappa^2\text{-}PPh_2MeIm)]$ [L = PPh_3 (**8**) or κ^1-PN (**9**)] by reaction of the PN ligand with $[RuHCl(PPh_3)_3]$ or [RuHCl(cod)(bpzm)], respectively. The molecular structure of **4b** and *fac*-**7a** was solved by an X-ray diffraction study. Complex **4b** has a dinuclear structure with two chloride bridges and two head-to-tail PN bridges. The derivative *fac*-**7a** is mononuclear. Both enantiomers — Δ and Λ — were observed in the same unit cell.

Introduction

Ruthenium(II) derivatives containing tertiary phosphane ligands are important precursors in catalytic processes, particularly hydrogenation.[1] For example, complexes of formula $[RuCl_2L_n]$, $[RuClHL_n]$ (n = 3, 4), $[RuCl_2(CO)L_3]$ or $[RuClH(CO)L_3]$ are efficient catalysts in the hydrogenation of alkenes,[2] alkynes,[2,3] aromatic heterocycles[4] or hydrocarbons,[5] aldehydes and ketones.[6] In many of these catalytic processes, cycles involving the decoordination of phosphanes or chlorides are involved.[1,2] For instance, $[RuCl_2(PPh_3)_3]$ is a classical starting point to give an active catalyst through phosphane[7] or chloride[8] dissociation. This process allows the coordination of substrates such as hydrogen or molecules that act as a hydrogen source, such as alcohols.[9] A theoretical alternative to the complete decoordination of a tertiary phosphane is the partial decoordination of a bidentate and hemilabile phosphane that probably causes only a minor effect on the electronic stability of the catalyst. With this possibility in mind, we envisaged the reaction of typical precursors like $[RuCl_2(PPh_3)_3]$ or $[RuClH(PPh_3)_3]$ with 2-(diphenylphosphanyl)-1-methyl-1*H*-imidazol[10] (PPh_2MeIm; Scheme 1), in different molar ratios, to obtain potential catalyst precursors with different structures and nuclearities. In order to compare our results and obtain complexes that are free of triphenylphosphane, we also used as starting materials $[RuCl_2(cod)(bpzm)]$

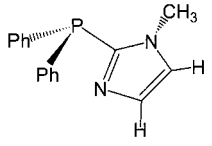

Scheme 1. PPh_2MeIm ligand

[a] Departamento de Química, Facultad de Ciencias, Universidad de Burgos,
Pza Misael Bañuelos s/n, 09001 Burgos, Spain
[b] Departamento de Química Inorgánica, Orgánica y Bioquímica, Universidad de Castilla-La Mancha,
13071 Ciudad Real, Spain
[c] Servicios Xerais de Apoio à Investigación, Universidade da Coruña,
Campus da Zapateira s/n, 15071 A Coruña, Spain

  DOI: 10.1002/ejic.200300892

[cod = 1,5-cyclooctadiene, bpzm = bis(pyrazol-1-yl)methane] and $[RuCl_2(p\text{-cymene})]_2$ as halide precursors and [RuClH(cod)(bpzm)] as a hydride.[11] In contrast to the widely used phosphane 2-(diphenylphosphanyl)pyridine,[12] the use of PPh_2MeIm as a bidentate ligand offers a more strained bite angle. This situation can favour the partial decoordination of the phosphane group.

Results and Discussion

The following discussion concerns the synthesis and characterisation of the new Ru^{II} derivatives containing the hemilabile ligand PPh_2MeIm (PN). The discussion is divided according to the Ru species used as the starting material.

Reaction of PPh_2MeIm with $[RuCl_2(PPh_3)_3]$ − X-ray structure of $[(PPh_3)ClRu(\mu\text{-}Cl)_2(\mu^2\text{-}P,N\text{-}PPh_2MeIm)_2Ru(PPh_3)Cl]\cdot CH_2Cl_2$

The reaction of $[RuCl_2(PPh_3)_3]$ with the ligand PN was studied in different molar ratios and this led to the formation of different complexes containing either one, two or three ligands bonded to the ruthenium centre. When $[RuCl_2(PPh_3)_3]$ was heated under reflux with 1 equiv. of PN in CH_2Cl_2 the polyphosphane complex **1** was isolated in 89% yield [Equation (1)].

$$[RuCl_2(PPh_3)_3] + PN \rightarrow [RuCl_2(PPh_3)_2(\kappa^2\text{-}PN)]\,(\mathbf{1}) + PPh_3 \qquad (1)$$

The conductivity data indicate that **1** is a neutral molecule. The $^{31}P\{^1H\}$ NMR spectrum (in $CDCl_3$; see Table 1) of **1** consists of an AMX pattern with two *cis* ^2J ($^2J_{A,M}$ and $^2J_{A,X}$) and one *trans* ^2J ($^2J_{M,X}$) coupling constants. These data are in agreement with a *mer* disposition of the three P atoms. The high-field doublet of doublets [δ = −22.2 ppm (P_X)] is consistent with the formation of a four-membered chelate ring in the PN ligand.[13] The IR spectrum of complex **1** shows a single absorption band at 326 cm^{-1}, which is characteristic of ν(Ru−Cl) with mutual *trans*-chloride ions.[14,15] The FAB^+ mass spectrum is in complete agreement with the expected fragmentation pattern and contains a peak corresponding to the fragment $[RuCl(PPh_3)_2(PN)]^+$ at m/z = 927, which is the result of chloride loss from **1**. In subsequent steps, the loss of PPh_3 gives $[RuCl(PPh_3)(PN)]^+$ (m/z = 665), and $[RuCl(PN)]^+$ (m/z = 403). On the basis of these data, the structure of **1**, which must be present as a mixture of enantiomers, is believed to be that shown in Scheme 2.

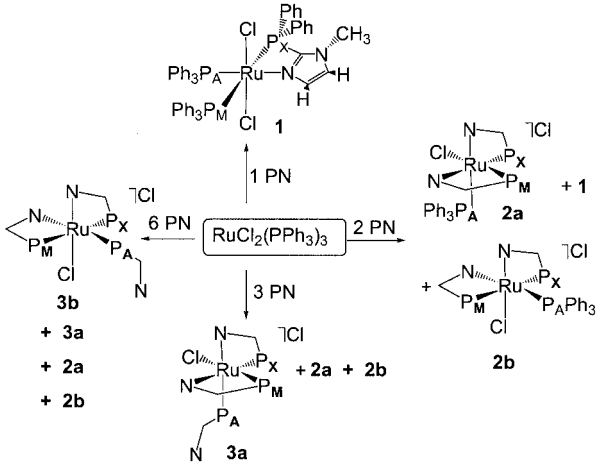

Scheme 2. Reaction scheme for the system $[RuCl_2(PPh_3)_3]/n$PN (n = 1, 2, 3, 6)

The reactions of $[RuCl_2(PPh_3)_3]$ with 2, 3 and 6 equiv. of the ligand PN were also investigated. These reactions led to the formation of four new complexes, as deduced from the corresponding $^{31}P\{^1H\}$ NMR spectra. The results can be summarised as follows (see Scheme 2): (i) When the Ru/PN ratio was 1:2, complex **1** was formed along with two new

Table 1. $^{31}P\{^1H\}$ NMR chemical shifts for the new complexes

Complex	Solvent	Spin system	δ [ppm]			J [Hz]		
			P_A	P_M or P_B	P_X	$^2J_{AM}$ or $^2J_{AB}$	$^2J_{AX}$	$^2J_{MX}$
mer-**1**	$CDCl_3$	AMX	43.70 dd	33.2 dd	−22.21 dd	29.00	32	322.15
fac-**2a**	$CDCl_3$	AMX	52.44 pt	7.55 pt	5.58 pt	36.01	28.2	27.51
mer-**2b**	$CDCl_3$	AMX	58.30 pt	−5.87 dd	−18.24 dd	31.73	26.3	304.02
fac-**3a**	$CDCl_3$	AMX	45.37 pt	15.91 pt	3.78 pt	32.02	33.6	32.03
mer-**3b**	$CDCl_3$	AMX	52.20 pt	−7.70 dd	−13.80 dd	31.31	28	312.81
4a	$CDCl_3$	AB	48.80 d	44.57 d	−	36.13	−	−
4b	$CDCl_3$	AM	68.09 d	19.43 d	−	36.63	−	−
4c	$CDCl_3$	AM	42.11 d	−1.12 d	−	25.32	−	−
5	$[D_6]$acetone[a]	AM	51.85 d	3.35 d	−	32.02	−	−
fac-**6a**[b]	$[D_6]$acetone	A_3	13.21 s	−	−	−	−	−
mer-**6b**[b]	$[D_6]$acetone	AMX	20.70 t	3.67[c] dd	−3.61[c] dd	26.93	26.91	290.52
fac-**7a**	$[D_6]$acetone	A_3	13.21 s	−	−	−	−	−
mer-**7b**	$[D_6]$acetone	AMX	20.70 t	3.67[c] dd	−3.61[c] dd	26.91	26.92	290.53
mer-**8**	C_6D_6	AMX	70.23 pt	53.82 dd	−14.90 dd	32.03	29.73	285.02
mer-**9**	C_6D_6	AMX	58.30 pt	40.49 dd	−10.00 dd	32.11	26.91	293.11

[a] At −90 °C. [b] The signal for the PF_6^- counteranion appears at δ = −143.2 (sept, $^1J_{F,P}$ = 708 Hz) ppm. [c] The assignment of P_M and P_X could be reversed.

complexes (**2a** and **2b**). (ii) When the ratio was 1:3, complex **1** was not formed but **2a**, **2b** and a new complex (**3a**) were observed in the reaction medium. (iii) The reaction with a ratio of 1:6 led to the formation of **2a**, **2b**, **3a** and a new derivative (**3b**).

We were able to deduce the structures of the four new complexes with the help of information obtained from a $^{31}P,^{31}P$ COSY experiment in $CDCl_3$ on a sample of the material formed in the reaction with the 1:6 ratio, which contained the four new derivatives (see Figure 1). The conclusions reached can be summarised as follows: (i) The spin system of each derivative fits an AMX pattern. (ii) Compounds **2a** and **3a** exhibit a *fac-PPP* disposition. (iii) Compounds **2b** and **3b** exhibit a *mer-PPP* disposition. (iv) All of these new compounds have two four-membered chelate rings (PN ligand) and one monodentate phosphane ligand, as deduced from the existence of two high-field signals and a low-field resonance for each derivative.

From the point of view of stoichiometry, it seems reasonable that in the reaction with a 1:2 ratio, the replacement of two PPh_3 units by two PN ligands takes place with the concomitant loss of one chloride ligand from the ruthenium centre. In this case complexes **2a** and **2b** will be the *fac* and *mer* isomers with the stoichiometry $[RuCl(PPh_3)(\kappa^2\text{-}P,N\text{-}PPh_2MeIm)_2]Cl$. These compounds contain one PPh_3 group, which can be removed by another molecule of PN when larger amounts of the ligand are used. This change leads to complexes **3a** and **3b** and these are the corresponding *fac* and *mer* isomers of stoichiometry $[RuCl(\kappa^1\text{-}P\text{-}PPh_2MeIm)(\kappa^2\text{-}P,N\text{-}PPh_2MeIm)_2]Cl$. The structures of the new derivatives, which are consistent with the data obtained, are shown in Scheme 2.

Attempts were made to obtain crystals of **1** from a dichloromethane/hexane mixture (1:1) in order to carry out an X-ray structure determination. Unexpectedly, the crystals obtained corresponded to the dinuclear species $[(PPh_3)ClRu(\mu\text{-}Cl)_2(\mu^2\text{-}P,N\text{-}PPh_2MeIm)_2Ru(PPh_3)Cl]$ (**4b**) as a dichloromethane solvate. The ORTEP plot of **4b** is shown in Figure 2, a selection of bond lengths and angles are given in Table 2. Other crystallographic data are given in the Exp. Sect. The complex has a dinuclear structure with two chloride bridges and two other head-to-tail axial PN bridges. The two metal centres are in a slightly distorted octahedral geometry as a consequence of the bridge strain, which is exemplified by the N(1)−Ru(1)−Cl(1) (86.04°) and N(1)−Ru(1)−Cl(1A) (82.80°) angles. The two terminal positions for each of the ruthenium atoms are occupied by one Cl and one PPh_3 ligand.

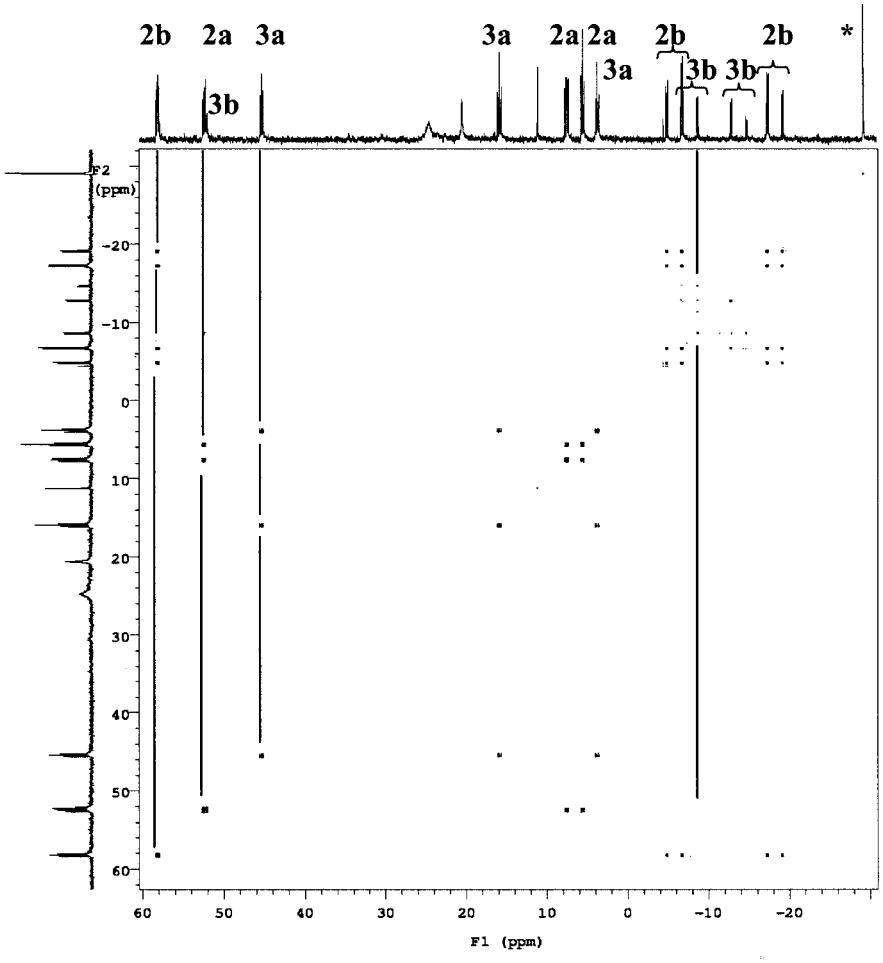

Figure 1. $^{31}P,^{31}P$ COSY spectrum (161.923 MHz) in $CDCl_3$ at room temperature for a sample of the reaction between $[RuCl_2(PPh_3)_3]$ and PMe_2MeIm in a 1:6 ratio; * indicates free PN

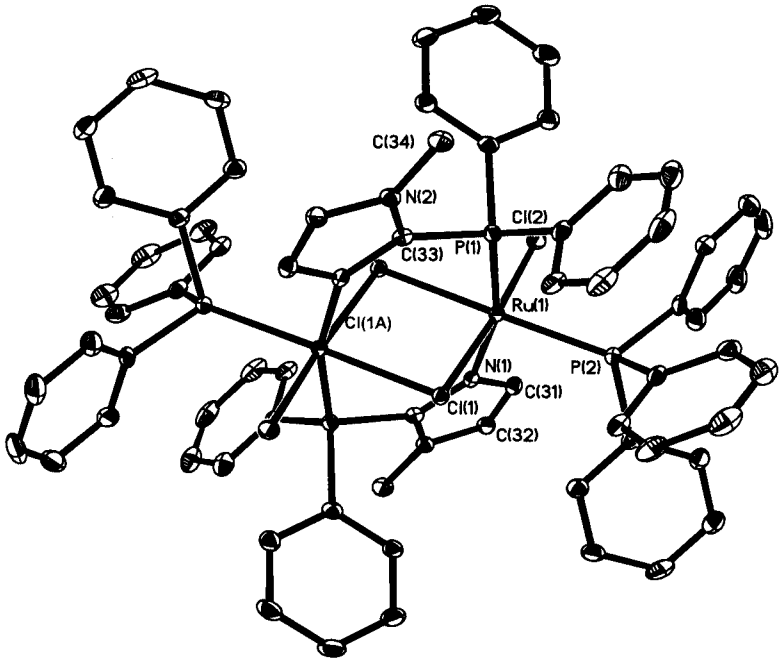

Figure 2. ORTEP plot of **4b**, showing atom labelling; hydrogen atoms have been omitted for clarity

Table 2. Selected bond lengths [Å] and angles [°] for **4b·CH_2Cl_2** and *fac*-**7a·$(CH_3)_2CO$** with estimated standard deviations in parentheses

4b·CH_2Cl_2			
Ru(1)−N(1)	2.146(3)	N(1)−Ru(1)−P(1)	164.83(7)
Ru(1)−P(1)	2.2929(9)	N(1)−Ru(1)−P(2)	93.92(7)
Ru(1)−P(2)	2.2967(9)	P(1)−Ru(1)−P(2)	100.81(3)
Ru(1)−Cl(1)	2.3878(8)	N(1)−Ru(1)−Cl(1)	86.04(7)
Ru(1)−Cl(2)	2.3987(8)	P(1)−Ru(1)−Cl(1)	89.47(3)
Ru(1)−Cl(1A)	2.4387(8)	P(2)−Ru(1)−Cl(1)	93.40(3)
P(1)−C(25)	1.832(3)	N(1)−Ru(1)−Cl(2)	87.43(7)
P(1)−C(19)	1.840(3)	P(1)−Ru(1)−Cl(2)	95.57(3)
P(1)−C(33)	1.861(3)	P(2)−Ru(1)−Cl(2)	92.04(3)
P(2)−C(13)	1.827(3)	Cl(1)−Ru(1)−Cl(2)	171.77(3)
P(2)−C(1)	1.848(3)	N(1)−Ru(1)−Cl(1A)	82.80(7)
P(2)−C(7)	1.852(3)	P(1)−Ru(1)−Cl(1A)	82.76(3)
		P(2)−Ru(1)−Cl(1A)	174.72(3)
		Cl(1)−Ru(1)−Cl(1A)	90.50(3)
		Cl(2)−Ru(1)−Cl(1A)	83.71(3)
		Ru(1)−Cl(1)−Ru(1A)	89.50(3)
fac-**7a·$(CH_3)_2CO$**			
Ru(1)−N(6)	2.140(2)	N(2)−Ru(1)−P(1)	68.74(6)
Ru(1)−N(4)	2.160(2)	N(4)−Ru(1)−P(2)	68.59(6)
Ru(1)−N(2)	2.173(2)	N(6)−Ru(1)−P(3)	69.04(7)
Ru(1)−P(1)	2.2954(8)	N(2)−C(13)−P(1)	105.50(18)
Ru(1)−P(3)	2.2990(9)	N(6)−C(45)−P(3)	104.58(18)
Ru(1)−P(2)	2.2995(8)	N(4)−C(29)−P(2)	105.28(18)

The Ru(1)−Ru(1A) distance is only 3.398 Å and is intermediate between those typically observed in complexes with $Ru^{II}(\mu\text{-}Cl)_2Ru^{II}$ bridges (but without an Ru−Ru bond, 3.68−3.91 Å)[11b,16] and those found in derivatives that do contain an Ru−Ru bond {e.g. 2.93 Å in $[RuCl_2(\mu^2\text{-}Cl_2)(\mu^2\text{-}dppm)RuCl_2]$}.[17] The presence of the two additional PCN bridges can lead to shortening of this distance, a situation that has been observed in other dinuclear Ru derivatives with additional short bridges.[18]

In addition, the distances between each of the chloride bridging ligands and each of the ruthenium atoms are asymmetric, with *d*[Ru(1)−Cl(1)] = 2.3878 Å and *d*[Ru(1A)−Cl(1)] = 2.4387 Å. This indicates a greater elongation of the μ-Cl−Ru bonds *trans* to PPh_3 in comparison to those *trans* to Cl^-. This situation is in keeping with the higher *trans* influence of a P-donor ligand than a chloride ligand.[18,19]

In order to understand the unexpected transformation of complex **1**, we monitored the evolution of a $CDCl_3$ solution of **1** during 3 d by $^{31}P\{^1H\}$ NMR spectroscopy. This experiment indicated that **1** undergoes a slow rearrangement in solution. The final $^{31}P\{^1H\}$ NMR spectrum is very complicated and shows the presence of several complexes (see Figure 3). A $^{31}P,^{31}P$ COSY experiment allowed each group of coupled signals to be correlated and indicated five independent spin systems and a singlet.

In this spectrum the resonances of **2a** and **2b** can be seen along with those of **4b**, which corresponds to an AM spin system (two doublets at δ = 19.43 and 68.09 ppm). The former of these signals can be assigned to a bridging coordination mode of the PN ligand on the basis of literature data.[20] The second doublet must correspond to coordinated PPh_3. Two additional spin systems can also be observed in the spectrum. Both of these have an AM pattern

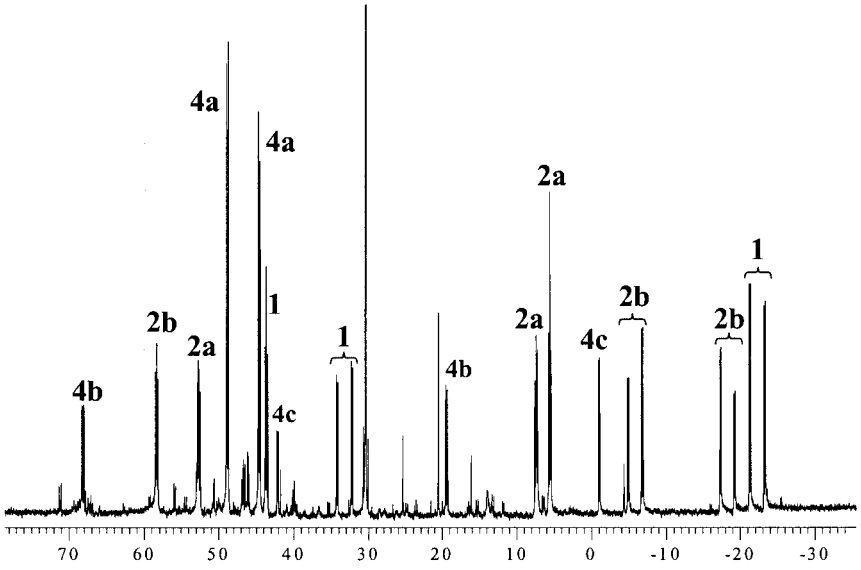

Figure 3. $^{31}P\{^{1}H\}$ NMR spectrum (161.923 MHz) in $CDCl_3$ at room temperature for a sample of **1** after 3 d in solution

with coupling constants typical of two P atoms in a *cis* disposition. The pair of signals for one complex, **4a**, have chemical shifts that do not correspond to either a chelating or bridging coordination of the PN ligand. Consequently, the PN ligand must exhibit monodentate coordination. One of the resonances of the other derivative, **4c**, indicates a chelating coordination. Considering this information we propose the structures indicated in Scheme 3 for complexes **4a** and **4c**. These structures are also reasonable in terms of the evolution of complex **1** after the loss of one PPh_3 ligand (see below). In the NMR spectrum there is also an intense singlet at $\delta = 30.3$ ppm, which can be assigned to $[RuCl_2(PPh_3)_3]$ — probably in equilibrium with free PPh_3.[21] According to the stoichiometry of the derivatives formed from **1**, both species must exist in the reaction medium (Scheme 3).

Although we do not have direct proof, we think that a reasonable mechanism for the dimerisation of **1** to **4a**, **4b** and **4c** is that shown in Scheme 4. This process would be favoured by the hemilabile character of the PN ligand and may involve the following steps: (i) Dissociation of one PPh_3 ligand. (ii) Partial dissociation of the PN ligand as a consequence of the strain in the four-membered ring and formation of two chloride bridges. Such a change leads to the formation of **4a**. The spontaneous dissociation of one PPh_3 group[22] and the consequent formation of chloride bridges[21b,23] has been reported for $[RuCl_2(PPh_3)_3]$. The coordination of the N atom to occupy the vacancy on each metal centre could take place in two ways, either to produce PN bridges between the two metal centres to give **4b**, or to regenerate a four-membered chelate ring on each metal atom to give **4c**.

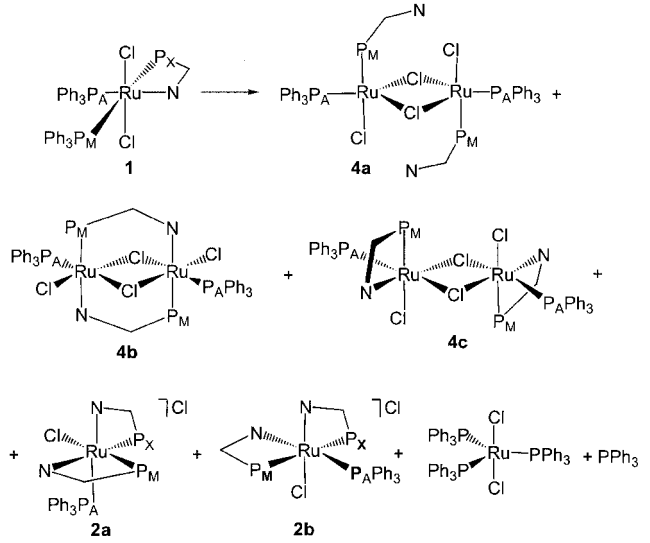

Scheme 3. Products formed after the evolution of **1** in solution

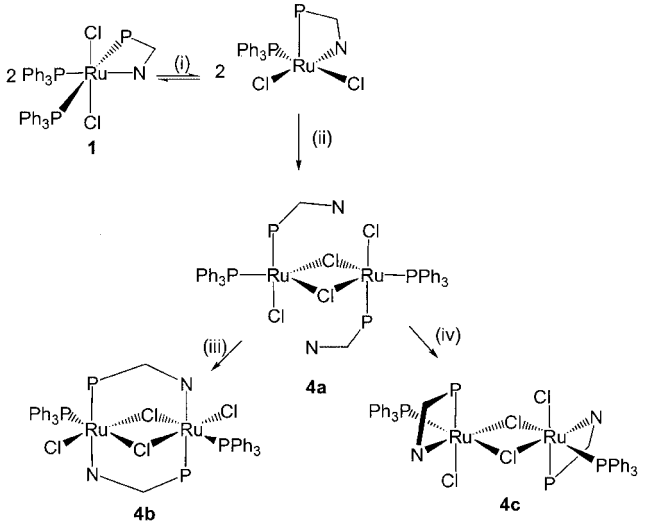

Scheme 4. Mechanism proposed for the dimerisation of **1**

Reaction of PPh_2MeIm with $[RuCl_2(cod)(bpzm)]$

In the previous reactions between the PN ligand and $[RuCl_2(PPh_3)_3]$ we obtained a rich variety of products that included not only mononuclear species with different amounts of the PN ligand but also dinuclear derivatives. It is clear from these results that competition between the incoming ligand and PPh_3 is always present and frequently leads to the formation of product mixtures. Even when 6 equiv. of the PN ligand were used, the products that do not contain PPh_3 (**3a**, **3b**) were formed along with those containing 1 equiv. of the phosphane (**2a**, **2b**). Given these findings, we decided to use a starting material that did not contain the phosphane ligand and incorporated weakly coordinating ligands — $[RuCl_2(cod)(bpzm)]$ [cod = 1,5-cyclooctadiene, bpzm = bis(pyrazol-1-yl)methane]. It has been shown that both cod and bpzpm ligands are prone to replacement by PN donor ligands.[11a] When 2 equiv. of PPh_2MeIm were added to a suspension of this compound and the mixture heated under reflux in THF, the complex *cis*-*P*-$[RuCl_2(\kappa^1$-*P*-$PPh_2MeIm)(\kappa^2$-*P*,*N*-$PPh_2MeIm)]$ (**5**) was obtained as the only product [Equation (2)].

$$[RuCl_2(cod)(bpzm)] + 2\,PN \rightarrow cis\text{-}P\text{-}[RuCl_2(\kappa^1\text{-}PN)(\kappa^2\text{-}PN)]\,(\mathbf{5}) + cod + bpzm \quad (2)$$

The ^1H NMR spectrum at low temperature does not show any evidence of the presence of bpzm or cod ligands and signals for only two kinds of PN ligand were observed. The corresponding $^{31}P\{^1H\}$ NMR spectrum ([D_6]acetone) at room temperature contains two broad signals that must be due to some kind of fluxional process. In an attempt to obtain more information on the structure of the complex, a $^{31}P\{^1H\}$ NMR spectrum was recorded at low temperature (−90 °C) and an AM pattern was observed [δ = 3.35 (d) and 51.85 (d) ppm]. The high-field resonance can be assigned to a PN ligand with a chelating coordination mode while the lower-field signal belongs to a monodentate PN ligand. The $^2J_{P,P}$ value (32.02 Hz) is indicative of a *cis* disposition of the two atoms. Moreover, the FAB^+ mass spectrum shows a peak at *m*/*z* = 669 due to the cation $[RuCl(PN)_2]^+$, which is the result of the loss of one chloride ion from **5**. Two bands at 367 and 297 cm^{-1}, assigned to the stretching vibration modes of the $RuCl_2$ unit, were observed in the IR spectrum. It can be concluded from these data that the complex is a monomeric, pentacoordinate compound with one bidentate and one monodentate PN ligand in which the P atoms are in a *cis* disposition but can exchange their coordination modes at room temperature through a fast process.

Interestingly, the reaction of $[RuCl_2(cod)(bpzm)]$ with 3 equiv. of the ligand PN under reflux gave a precipitate that was identified as complex **3**, with no other compound being detected. Complex **3** was present as four diastereoisomers: the pair of enantiomers *fac*-**3a** and the pair *mer*-**3b** in a molar ratio of 4:1. As stated previously, these isomers were also obtained when $[RuCl_2(PPh_3)_3]$ was used as the starting material but always in a mixture with other derivatives (see Table 1 for the ^{31}P NMR spectroscopic data). The FAB^+ spectrum is consistent with the proposed formulation, as a peak corresponding to the cation of **3** is observed at *m*/*z* = 935. The rest of the peaks are in agreement with the loss of a chloride ion and two PN ligands in successive steps (see Exp. Sect.).

Reaction of PPh_2MeIm with $[RuCl_2(p\text{-cymene})]_2$ − X-ray Structure of *fac*-$[Ru(\kappa^2$-*P*,*N*-$PPh_2MeIm)_3](BF_4)_2\cdot(CH_3)_2CO$

Another goal of our study was the synthesis of derivatives of the type $[Ru(PN)_3]X_2$, with three chelate ligands. Such complexes would be expected to be chiral[24] and, considering the hemilabile character of the PN ligand, they could be interesting starting materials in catalytic or stoichiometric processes.[25] We succeeded in the synthesis of these compounds by using $[RuCl_2(arene)]_2$ (arene = *p*-cymene, benzene) as starting materials and adding silver salts to remove the chloride ions. In this way, the complexes $[Ru(\kappa^2$-*P*,*N*-$PPh_2MeIm)_3]X_2$ [X = PF_6 (**6**) and BF_4 (**7**)] were isolated after the addition of the ligand PPh_2MeIm to the solution obtained by treatment of a suspension of $[RuCl_2(arene)]_2$ in MeOH with $AgPF_6$ or $AgBF_4$, respectively, at room temperature [Equation (3)]. The same products were also formed upon treatment of $[RuCl_2(cod)(bpzm)]$ with the silver salt and the PN ligand, but in this case the reaction led to a mixture of derivatives. Consequently, the reaction outlined in Equation (3) is more convenient.

$$[RuCl_2(arene)]_2 + 4\,AgX + 6\,PN \rightarrow 2\,[Ru(\kappa^2\text{-}PN)_3]X_2 + 4\,AgCl \quad (3)$$

arene = *p*-cymene, X = PF_6 (**6**); arene = benzene, X = BF_4 (**7**)

In both cases the two pairs of stereoisomers, *fac* (**6a** and **7a**) and *mer* (**6b** and **7b**), were formed. The ^1H NMR spectra lack the characteristic signals of *p*-cymene or benzene. The $^{31}P\{^1H\}$ NMR spectrum of **6** exhibits the AM_6 pattern of the PF_6^- counteranion. Furthermore, a singlet for the *fac* stereoisomer (chemical shift of chelate coordination) and the AMX pattern of a *mer* stereoisomer are observed for both derivatives. Two signals at high field due to the *mer* form are typical of chelate coordination. However, the resonance at δ = 20.70 ppm could correspond to a chelating or bridging PN ligand, which means that the compound could be mono- or dinuclear in nature. In an effort to clarify this point, high-resolution mass spectra were obtained for **6** and **7**. Only the spectrum of compound **6** will be discussed as it is very similar to that of **7**. The spectrum displays a group of signals corresponding to the fragment $[\{Ru(PN)_3\}\{PF_6\}]^+$, whose most intense peak appears at *m*/*z* = 1045.2. In addition a signal at *m*/*z* = 450.13 was observed, which is consistent with the dicationic fragment $[\{Ru(PN)_3\}]^{2+}$, as deduced from the difference between the lines in this group of half a unit. The overall fragmentation pattern for this molecule is indicated in Scheme 5. No evidence for the existence of a dinuclear species was found in

the mass spectrum. Consequently, all the data indicate a mononuclear structure for both derivatives (Scheme 6).

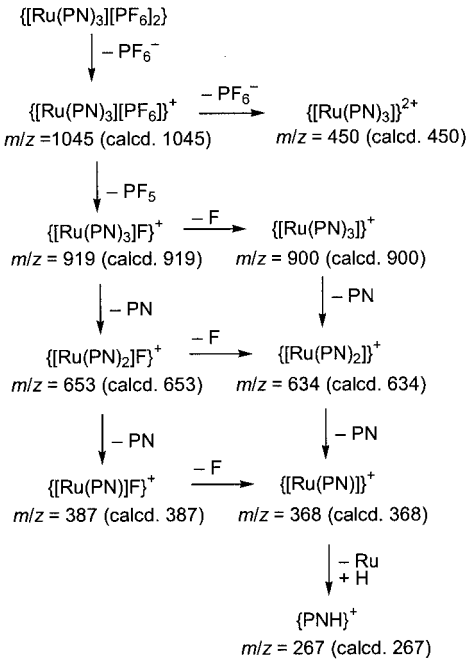

Scheme 5. Fragmentation pattern for **6**

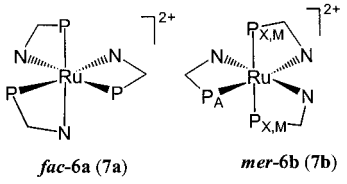

Scheme 6. Proposed structures for **6** and **7**

Finally, it was possible to crystallise the *fac* isomer of **7** (i.e. **7a**) as an acetone solvate and to determine its molecular structure by an X-ray diffraction study on a single crystal. The corresponding ORTEP plot is shown in Figure 4, selected bond lengths and angles are shown in Table 2 and crystallographic data are given in the Exp. Sect. The compound is mononuclear and exhibits a *fac* disposition of the three phosphorus atoms. Only the structure for the Δ isomer is shown in Figure 4a, although it should be noted that both the Δ and Λ enantiomers are present in the same unit cell (see Figure 4b).

At present, only one structure containing three four-membered PN chelate rings has been deposited with the CSD[26] and that corresponds to the complex [Ru(pyphos)$_3$](μ-Na$_2$)[Ru(pyphos)$_3$] in which each pseudo-octahedral ruthenium(II) centre has three PN chelating ligands [pyphos = 6-(diphenylphosphanyl)-2-pyridonate]. As in the case of **7a**, a *fac* disposition for the identical donor atoms was found.

A comparison between the free and the chelate-coordinated ligand in *fac*-**7a** reflects the fact that the P−C−N

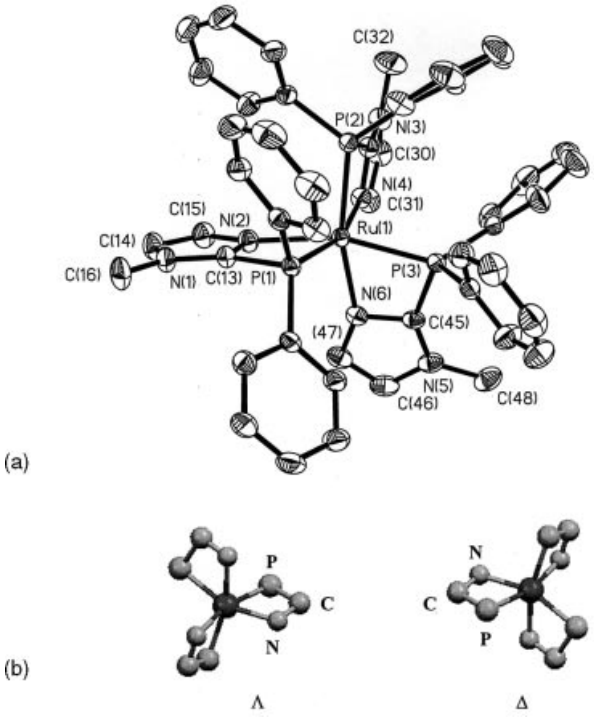

Figure 4. (a) ORTEP plot of the cation of the Δ enantiomer of *fac*-**7a**, showing the atom labelling; hydrogen atoms and phenyl groups have been omitted for clarity, as have counterions and solvent molecules; (b) ball-and-stick plots for *fac*-**7a**, showing both enantiomers

angle decreases with κ^2-*PN* coordination from 128.5(2)°[27] in the free ligand to about 105° in **7a**. Very similar angles (about 103°) are present in the previously mentioned [Ru(pyphos)$_3$] units. This situation can be seen as a consequence of the inherent strain associated with the four-membered chelate ring. Similarly, the Ru−N bonds are relatively long[28] and the bite angles of the PN donor ligands are small.

Hydride Complexes

We also tried to synthesise new hydride complexes containing the PPh_2MeIm ligand. In order to achieve this aim we used two types of hydride starting material, one containing PPh_3 and the other with more easily displaceable ligands — [RuHCl(PPh_3)$_3$] and [RuHCl(cod)(bpzm)].

When equivalent amounts of [RuHCl(PPh_3)$_3$] and PPh_2MeIm were mixed in toluene at 70 °C, *mer*-[RuHCl(PPh_3)$_2$(κ^2-*P,N*-PPh_2MeIm)] (**8**) was isolated in good yield [Equation (4)].

$$[RuHCl(PPh_3)_3] + PN \rightarrow mer\text{-}[RuHCl(PPh_3)_2(\kappa^2\text{-}PN)]\ (\mathbf{8}) + PPh_3 \quad (4)$$

The hydride region of the ^{1}H NMR (C_6D_6) spectrum of **8** shows a quadruplet at δ = −15.1 ppm ($^2J_{P,H}$ = 26.6, $^2J_{P,H}$ = 23.5, $^2J_{P,H}$ = 23.4 Hz) as the most characteristic signal. This relatively high-field chemical shift is typical for a hydride ion *trans* to an N atom, as reported in the litera-

ture,[29] and is in contrast to the lower-field chemical shift observed for hydride ions *trans* to Cl ligands.[11,30] The values of the three coupling constants, determined separately by selective $^1H\{^{31}P\}$ NMR decoupling experiments, correspond to a *cis* disposition of the hydride ion with respect to the three P atoms, which also means a *mer-PPP* disposition. The $^{31}P\{^1H\}$ NMR (C_6D_6) spectrum of **8** confirms the stereochemistry of the complex, since it consists of an AMX pattern with one *trans*-PP coupling constant between a PPh_3 and a chelating PPh_2MeIm group. Consequently, the spectroscopic data indicate the presence of the *mer* stereoisomer in solution (see Scheme 7). Obviously, complex **8** is isolated as a racemic mixture.

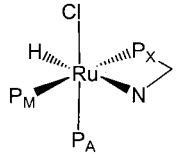

$P_A = P_M = PPh_3$, ***mer*-8**
$P_A = P_M = PPh_2MeIm$, ***mer*-9**

Scheme 7. Proposed structures of complexes **8** and **9**

An excess of the ligand PPh_2MeIm (6:1) was mixed with [RuHCl(cod)(bpzm)] in THF at −80 °C and the hydrido complex *mer*-[RuHCl(κ^1-*P*-PPh_2MeIm)$_2$(κ^2-*P*,*N*-PPh_2MeIm)] (**9**) was obtained [Equation (5)].

$$[RuHCl(cod)(bpzm)] + 6\,PN \rightarrow mer\text{-}[RuHCl(\kappa^1\text{-}PN)_2(\kappa^2\text{-}PN)]\,(\mathbf{9}) + cod + bpzm \quad (5)$$

The ^1H (C_6D_6) and $^{31}P\{^1H\}$ NMR (C_6D_6) spectra of **9** are completely analogous to those of **8**. Two of the phosphorus chemical shifts are typical of a monodentate coordination of the PN ligand while a resonance appearing at $\delta = -10$ ppm indicates the existence of a chelating PPh_2MeIm group. Consequently, the presence of the *mer* stereoisomer, as a racemic mixture, is again evident (see Scheme 7). The two PPh_3 ligands in compound **8** are monodentate PPh_3MeIm groups in **9**.

Conclusion

We have prepared new families of (polyphosphane)Ru complexes containing the ligand 2-(diphenylphosphanyl)-1-methyl-1*H*-imidazole. In the complexes described, three types of coordination modes for the N,P ligand have been found: *P*-monodentate, chelate and brigde. An unexpected rearrangement of [$RuCl_2$(Pn)(PPh_3)$_2$] that leads, among others, to the formation of dinuclear derivatives has been found. The formation of these species involves an Ru−N bond-breaking step that demonstrates the hemilabile behaviour of the ligand.

Experimental Section

General Comments: All manipulations were carried out under Ar using standard Schlenk techniques. Solvents (Merck) were dried and distilled under N_2 prior to use. [$RuCl_2(PPh_3)_3$],[31] [$RuHCl(PPh_3)_3$],[32] [$RuCl_2$(bpzm)(cod)],[33] [RuHCl(bpzm)-(cod)],[33] [$RuCl_2$(*p*-cymene)]$_2$,[34] [$RuCl_2(C_6H_6)$]$_2$ [34] and PPh_2MeIm[27] were prepared according to literature procedures. NMR spectra were recorded at room temperature (ca. 22 °C), unless otherwise stated, with a Varian Unity Inova-400 (400 MHz for ^1H; 161.9 MHz for ^{31}P; 100.6 MHz for ^{13}C) or with a Varian Unity-300 (300 MHz for ^1H; 121.4 MHz for ^{31}P; 75.4 MHz for ^{13}C) spectrometer. ^1H NMR shifts are referenced to the residual proton of the solvent as internal standard. All ^{31}P shifts were referenced internally to H_3PO_4. The ^{31}P,^{31}P COSY spectrum was acquired using a 30604 Hz spectral width; 24 transients were collected for each 240 increments. A 1 s relaxation delay, a 45° pulse width, and a 0.20 s acquisition time were used. IR spectra were recorded with a Nicolet Impact 410 spectrophotometer as KBr pellets or with a Perkin−Elmer 883 (4000−200 cm^{-1} range) as Nujol mulls. Conductivity measurements were made at 25 °C with freshly prepared 10^{-3} M solutions of the complex in acetone, using a CRISON 522 conductimeter. Molar conductivities (Λ_M) are given in units of $\Omega^{-1}\cdot mol^{-1}\cdot cm^2$. Elemental analyses were performed with a LECO CHNS932 microanalyser. FAB^+ mass spectra were recorded at the University of Zaragoza with a VG AutoSpec or at the University of Burgos with a Micromass Autospec by Liquid Secondary Ion Mass Spectrometry (LSMIS+) with Cs and NBA ions as the matrix.

***trans*,*mer*-[$RuCl_2(PPh_3)_2$(κ^2-*P*,*N*-PPh_2MeIm)] (1):** PPh_2MeIm (29.5 mg, 0.11 mmol) was added to a suspension of [$RuCl_2(PPh_3)_3$] (106 mg, 0.11 mmol) in 20 mL of CH_2Cl_2 (1:1). The resulting mixture was stirred and refluxed for 16 h. The original suspension became a red solution, which was concentrated to dryness. The orange solid obtained was washed with pentane (15 mL) and then with diethyl ether (3 × 15 mL) to remove any residual PPh_3. Finally, it was dried under vacuum. Yield: 89% (94.8 mg). The product is soluble in $CHCl_3$, CH_2Cl_2 and acetone. It decomposes in solution under air, giving rise to a green-brownish suspension after some minutes. However, it can be stored, as a solid, under nitrogen for months without appreciable decomposition. $C_{52}H_{45}Cl_2N_2P_3Ru$ (962.85): calcd. C 64.87, H 4.71, N 2.91; found C 65.11, H 4.80, N 2.83. FAB^+: *m*/*z* = 927 [M − Cl]$^+$, 665 [M − Cl − PPh_3]$^+$, 403 [M − Cl − 2PPh_3]$^+$.^1H NMR (400 MHz, $CDCl_3$, room temp.): δ = 7.9−6.7 (m, 40 H, 8 Ph), 6.6 (s, 1 H, H-Im), 5.56 (s, 1 H, H-Im), 3.0 (s, 3 H, Me-Im) ppm.$^{13}C\{^1H\}$ NMR (100.6 MHz, $CDCl_3$, room temp.): δ = 150−125 (m, 49 C, 8 Ph, C^2-Im), 130.7 (s, 1 C, *C*H-Im), 123.4 (s, 1 C, *C*H-Im), 34.2 (s, 1 C, Me-Im) ppm. $^{31}P\{^1H\}$ NMR: See Table 1. Λ_M (25 °C, acetone) = 10.35 $\Omega^{-1}\cdot mol^{-1}\cdot cm^2$. IR (nujol mull): $\tilde{\nu}$ = 326 cm^{-1} [ν(*trans*-$RuCl_2$)].

Reaction of [$RuCl_2(PPh_3)_3$] with PPh_2MeIm in a 1:2 Molar Ratio: The procedure is similar to that used for obtaining compound **1**. PPh_2MeIm (59 mg, 0.22 mmol) was added to a suspension of [$RuCl_2(PPh_3)_3$] (106 mg, 0.11 mmol) (2:1) in 20 mL of CH_2Cl_2. The resulting mixture was stirred and refluxed for 16 h. The original suspension became a red solution, which was concentrated to dryness. The orange solid obtained was washed with pentane (15 mL) and then with diethyl ether (3 × 10 mL) to remove any residual PPh_3 or PPh_2MeIm. Finally, it was dried under vacuum. The resulting mixture was studied by $^{31}P\{^1H\}$ NMR spectroscopy, and the following compounds were detected (see Table 1 for the $^{31}P\{^1H\}$ NMR spectroscopic data): **1**, *fac*-[RuCl(PPh_3)(κ^2-*P*,*N*-

$PPh_2MeIm)_2$]Cl (**2a**) and *mer*-[RuCl(PPh_3)(κ^2-*P*,*N*-$PPh_2MeIm)_2$]Cl (**2b**).

Reaction of [$RuCl_2(PPh_3)_3$] with PPh_2MeIm in a 1:3 Molar Ratio: The procedure is similar to that described for the 1:2 molar ratio. Amounts are as follows: PPh_2MeIm (88.6 mg, 0.33 mmol), [$RuCl_2(PPh_3)_3$] (106 mg, 0.11 mmol) and 20 mL of CH_2Cl_2. The resulting mixture was studied by $^{31}P\{^1H\}$ NMR spectroscopy and the following compounds were detected (see Table 1 for the $^{31}P\{^1H\}$ NMR spectroscopic data): **2a**, **2b** and *fac*-[RuCl(κ^1-*P*-PPh_2MeIm)(κ^2-*P*,*N*-$PPh_2MeIm)_2$]Cl (**3a**).

Reaction of [$RuCl_2(PPh_3)_3$] with PPh_2MeIm in a 1:6 Molar Ratio: The procedure is similar to that described for the 1:2 molar ratio. Amounts are as follows: PPh_2MeIm (177 mg, 0.66 mmol), [$RuCl_2(PPh_3)_3$] (106 mg, 0.11 mmol) and 30 mL of CH_2Cl_2. The resulting mixture was studied by $^{31}P\{^1H\}$ NMR spectroscopy, and the following compounds were detected (see Table 1 for the $^{31}P\{^1H\}$ NMR spectroscopic data): **2a**, **2b**, **3a** and *mer*-[RuCl(κ^1-*P*-PPh_2MeIm)(κ^2-*P*,*N*-$PPh_2MeIm)_2$]Cl (**3b**).

[RuCl(κ^1-*P*-PPh_2MeIm)(κ^2-*P*,*N*-$PPh_2MeIm)_2$]Cl (3): PPh_2MeIm (139.9 mg, 0.526 mmol) was added to a suspension of [$RuCl_2$(cod)(bpzm)] (75 mg, 0.175 mmol) in THF (30 mL) (3:1). The resulting mixture was stirred and refluxed for 6 h. A yellow solid was obtained which, after filtering and washing with *n*-pentane (3 × 10 mL), was dried under vacuum. Yield: 72% (123 mg). The product is soluble in CH_2Cl_2 and $CHCl_3$. $C_{48}H_{45}Cl_2N_6P_3Ru$ (970.83): calcd. C 59.39, H 4.67, N 8.66; found C 59.22, H 4.81, N 8.57. FAB^+: *m*/*z* = 935 $[M]^+$, 900 $[M - Cl]^+$, 634 $[M - Cl - PN]^+$, 450 $[M - Cl^-]^{2+}$, 368 $[M - Cl - 2\ PN]^+$, 267 $[PN + H^+]^+$.

***fac*-[RuCl(κ^1-*P*-PPh_2MeIm)(κ^2-*P*,*N*-$PPh_2MeIm)_2$]Cl (3a):** ^1H NMR (400 MHz, $CDCl_3$, room temp.): δ = 9.0−6.2 (m, 36 H, 6 Ph, 3 CH-Im), 3.63 (s, 3 H, Me-Im), 3.22 (s, 3 H, Me-Im), 2.74 (s, 3 H, Me-Im) ppm.

***mer*-[RuCl(κ^1-*P*-PPh_2MeIm)(κ^2-*PN*-$PPh_2MeIm)_2$]Cl (3b):** ^1H NMR (400 MHz, $CDCl_3$, room temp.): δ = 9.0−6.2 (m, 36 H, 6 Ph, 3 CH-Im), 3.79 (s, 3 H, Me-Im), 3.26 (s, 3 H, Me-Im), 2.68 (s, 3 H, Me-Im) ppm. $^{31}P\{^1H\}$ NMR: See Table 1.

[(PPh_3)(κ^1-*P*-PPh_2MeIm)ClRu(μ-Cl)$_2$Ru(PPh_3)(κ^1-*P*-PPh_2MeIm)Cl] (4a): This compound was detected by $^{31}P\{^1H\}$ NMR spectroscopy in a solution of **1** in $CDCl_3$ after standing for 3 d at room temperature.

[(PPh_3)ClRu(μ-Cl)$_2$(μ^2-*P*,*N*-$PPh_2MeIm)_2$Ru(PPh_3)Cl] (4b): This compound was obtained as a crystalline solid from a solution of **1** in CH_2Cl_2/hexane under nitrogen and it was also detected by $^{31}P\{^1H\}$ NMR spectroscopy in a solution of **1** in $CDCl_3$ after standing at room temperature for 3 d.

[(PPh_3)(κ^2-*PN*-PPh_2MeIm)ClRu(μ-Cl)$_2$Ru(PPh_3)(κ^2-*PN*-PPh_2MeIm)Cl] (4c): This compound was detected by $^{31}P\{^1H\}$ NMR spectroscopy in a solution of **1** in $CDCl_3$ after standing at room temperature for 3 d.

***cis*-*P*-[$RuCl_2$(κ^1-*P*-PPh_2MeIm)(κ^2-*P*,*N*-PPh_2MeIm)] (5):** PPh_2-MeIm (66 mg, 0.24 mmol) was added to a suspension of [$RuCl_2$(cod)(bpzm)] (53.6 mg, 0.12 mmol) in 30 mL of THF (2:1). The resulting mixture was stirred and refluxed for 14 h, then filtered and the resulting solution concentrated to dryness. The pale-green solid obtained was washed with diethyl ether (2 × 10 mL) and finally dried under vacuum. Yield: 68% (60 mg). The compound is soluble in acetone and $CHCl_3$. $C_{32}H_{30}Cl_2N_4P_2Ru$ (704.55): calcd. C 54.55, H 4.29, N 7.95; found C 54.62, H 4.33, N 8.21. FAB^+: *m*/*z* = 669 $[M - Cl]^+$, 403 $[M - Cl - PN]^+$. ^1H NMR (300 MHz, [D_6]acetone, room temp.): δ = 8.0−6.8 (m, 24 H, 4 Ph, 4 CH-Im), 2.97 (s, 3 H, Me-Im) 2.81 (s, 3 H, Me-Im) ppm. $^{31}P\{^1H\}$ NMR: See Table 1. IR (Nujol mull): $\tilde{\nu}$ = 367, 297 cm^{-1} [ν(RuCl)].

[Ru(κ^2-*P*,*N*-$PPh_2MeIm)_3$][PF_6]$_2$ (6): $AgPF_6$ (253 mg, 1.00 mmol) was added to a suspension of [$RuCl_2$(*p*-cymene)]$_2$ (153 mg, 0.25 mmol) in 8 mL of MeOH at room temperature (4:1). The mixture was protected from light and stirred for 30 min. It was then filtered and the precipitated AgCl was removed. PPh_2MeIm (266.1 mg, 1.00 mmol) was then added to the previous orange solution, and the resulting mixture was stirred at room temperature for 3 h. The solvent was removed under vacuum and the obtained oil was transformed into a solid with pentane after stirring and scratching. The yellow solid was filtered and dried under vacuum. It is soluble in acetone. Yield: 87% relative to the ligand (344.7 mg). When the reaction was performed with 1.50 mmol of the PN ligand, other products besides **6** were formed. The compound was obtained as a mixture of four diastereoisomers: the pair of *fac* enantiomers **6a** and the *mer* pair **6b**. $C_{48}H_{45}F_{12}N_6P_5Ru$ (1189.9): calcd. C 48.45, H 3.81, N 7.06; found C 48.14, H 3.93, N 7.32. FAB^+ (see also Scheme 5): *m*/*z* = 1045 $[M - PF_6]^+$, 450 $[M - 2\ PF_6^-]^{2+}$, 919 $[M - PF_6^- - PF_5]^+$, 900 $[M - PF_6^- - PF_6]^+$, 653 $[M - PF_6^- - PF_5 - PN]^+$, 634 $[M - PF_6^- - PF_6 - PN]^+$, 387 $[M - PF_6^- - PF_5 - 2\ PN]^+$, 368 $[M - PF_6^- - PF_6 - 2\ PN]^+$, 267 $[PN + H^+]^+$.

6a: ^1H NMR (400 MHz, [D_6]acetone, room temp.): δ = 8.2−6.6 (m, 36 H, 6 Ph, 6 CH-Im), 3.72 (s, 3 H, Me-Im) 3.63 (s, 3 H, Me-Im) 3.57 (s, 3 H, Me-Im) ppm.

6b: ^1H NMR (400 MHz, [D_6]acetone, room temp.): δ = 8.2−6.6 (m, 36 H, 6 Ph, 6 CH-Im), 3.61 (s, 9 H, Me-Im) ppm. $^{31}P\{^1H\}$ NMR: See Table 1. IR (KBr): $\tilde{\nu}$ = 838 cm^{-1} [ν(P−F), PF_6^-].

[Ru(κ^2-*P*,*N*-$PPh_2MeIm)_3$][BF_4]$_2$ (7): $AgBF_4$ (389.4 mg, 2.00 mmol) was added to a suspension of [$RuCl_2$(benzene)]$_2$ (250 mg, 0.5 mmol) in 15 mL of MeOH at room temperature (4:1). The mixture was protected from light and stirred for 30 min. Then it was filtered and the precipitated AgCl was removed. PPh_2MeIm (532.2 mg, 2.00 mmol) was added to the previous orange solution, and the resulting mixture was stirred at room temperature for 3 h. The solvent was removed under vacuum and the obtained oil was transformed into a solid with pentane after stirring and scratching. The yellow solid was filtered and dried under vacuum. It is soluble in acetone. Yield: 76% relative to the ligand (535.8 mg). When the reaction was performed with 3.00 mmol of the PN ligand, other products besides **7** were formed. The compound was obtained as a mixture of four diastereoisomers: the pair of *fac* enantiomers **7a** and the *fac* pair **7b**. The *mer* enantiomers were crystallised from an Et_2O solution. $C_{48}H_{45}B_2F_8N_6P_3Ru$ (1073.5): calcd. C 53.70, H 4.23, N 7.83; found C 53.85, H 4.31, N 7.91. FAB^+: *m*/*z* = 987 $[M - BF_4^-]^+$, 450 $[M - 2\ BF_4^-]^{2+}$, 919 $[M - BF_4^- - BF_3]^+$), 900 $[M - BF_4^- - BF_4]^+$, 653$[M - BF_4^- - BF_3 - PN]^+$, 634 $[M - BF_4^- - BF_4 - PN]^+$, 387 $[M - BF_4^- - BF_3 - 2\ PN]^+$, 368 $[M - BF_4^- - BF_4 - 2\ PN]^+$, 267 $[PN + H^+]^+$. IR (KBr): $\tilde{\nu}$ = 1059 cm^{-1} [ν(B−F), BF_4^-], 544 [δ(FBF), BF_4^-].

7a: ^1H NMR (400 MHz, [D_6]acetone, room temp.): δ = 8.2−6.6 (m, 36 H, 6 Ph, 6 CH-Im), 3.72 (s, 3 H, Me-Im) 3.63 (s, 3 H, Me-Im) 3.57 (s, 3 H, Me-Im) ppm.

7b: ^1H NMR (400 MHz, [D_6]acetone, room temp.): δ = 8.2−6.6 (m, 36 H, 6 Ph, 6 CH-Im), 3.61 (s, 9 H, Me-Im) ppm. $^{31}P\{^1H\}$ NMR: See Table 1.

***mer*-[RuHCl(PPh$_3$)$_2$(κ^2-*P*,*N*-PPh$_2$MeIm)] (8):** PPh$_2$MeIm (20.4 mg, 0.077 mmol) was added to a suspension of [RuHCl(PPh$_3$)$_3$] (61.4 mg, 0.07 mmol) in 20 mL of toluene (1.1:1). The resulting mixture was stirred and heated to 70 °C for 4 h. The original violet suspension became a dark green solution and was concentrated to dryness. The green solid obtained was washed with pentane (15 mL) and dried under vacuum. Yield: 85% (55 mg). It is very air-sensitive and soluble in toluene and benzene. $C_{52}H_{46}ClN_2P_3Ru$ (928.4): calcd. C 67.27, H 4.99, N 3.02; found C 67.21; H 5.02, N 3.14. ^{1}H NMR (400 MHz, C_6D_6, room temp.): δ = 8.2−6.6 (m, 41 H, 8 Ph, 1 CH-Im), 5.95 (s, 1 H, CH-Im), 3.5 (s, 3 H, Me-Im), −15.1 (q, $^2J_{P,H}$ = 26.6, $^2J_{P,H}$ = 23.5, $^2J_{P,H}$ = 23.4 Hz, 1 H, Ru−H) ppm. ^{31}P{^{1}H} NMR: See Table 1.

***mer*-[RuHCl(κ^1-*P*-PPh$_2$MeIm)$_2$(κ^2-*P*,*N*-PPh$_2$MeIm)] (9):** PPh$_2$-MeIm (351.6 mg, 1.32 mmol) was added to a suspension of [RuHCl(cod)(bpzm)] (86.6 mg, 0.22 mmol) in 20 mL of THF at −80 °C (6:1). The resulting mixture was stirred at this temperature for 45 min and at room temperature for furthe 30 min. The original suspension turned to a yellow solution with a small amount of solid in suspension. This mixture was concentrated to dryness and the yellow solid obtained was washed with diethyl ether (2 × 10 mL) to remove any bpzm, cod and unreacted ligand, and finally dried under vacuum. Yield: 73% (150 mg). The compound is very air-sensitive and soluble in C_6D_6, but it is insoluble in acetone. $C_{48}H_{46}ClN_6P_3Ru$ (936.39): calcd. C 61.57, H 4.95, N 8.97; found C 61.63, H 4.93, N 8.99. FAB$^+$: *m*/*z* = 935 [M − H$^-$]$^+$, 900 [M − H$^-$ − Cl]$^+$, 634 [M − H$^-$ − Cl − PN]$^+$, 450 [M − H$^-$ − Cl$^-$]$^{2+}$, 368 [M − H$^-$ − Cl − 2 PN]$^+$, 267 [PN + H$^+$]$^+$, 669 [M − H$^-$ − PN]$^+$, 403 [M − H$^-$ − 2 PN]$^+$.^{1}H NMR (400 MHz, C_6D_6, room temp.): δ = 8.4−6.4 (m, 36 H, 6 Ph, 6 CH-Im), 3.45 (s, 3 H, Me-Im), 2.97 (s, 3 H, Me-Im), 2.81 (s, 3 H, Me-Im), −14.8 (q, $^2J_{P,H}$ ≈ 25 Hz, 1 H, Ru-H) ppm. ^{31}P{^{1}H} NMR: See Table 1.

X-ray Diffraction: Suitable crystals of complexes **4b·CH$_2$Cl$_2$** (red block, dimensions 0.26 × 0.23 × 0.10 mm) and *fac*-**7a·(CH$_3$)$_2$CO** (yellowish prism, dimensions 0.50 × 0.30 × 0.30 mm) were used for the structure determination. X-ray data (Table 3) were collected using a Bruker SMART CCD area detector single-crystal diffractometer with graphite-monochromated Mo-K_α radiation (λ = 0.71073 Å) by the -ω scan method at 173(2) K (**4b**) or 296(2) (*fac*-**7a**). A total of 1271 frames of intensity data were collected for each compound. The first 50 frames were recollected at the end of data collection to monitor for decay. The crystals used for the diffraction studies showed a small amount of decomposition during data collection for **4b·CH$_2$Cl$_2$** (1.5%) and no decomposition for *fac*-**7a·(CH$_3$)$_2$CO**. The integration process yielded a total of 22750 reflections for **4b·CH$_2$Cl$_2$** and 28912 for *fac*-**7a·(CH$_3$)$_2$CO**, of which 7606 [*R*(int) = 0.0712] for **4b·CH$_2$Cl$_2$** and 11344 for *fac*-**7a·(CH$_3$)$_2$CO** were independent. Absorption corrections were applied using the SADABS[35] program (maximum and minimum transmission coefficients, 1.0000 and 0.809831 for **4b·CH$_2$Cl$_2$**). The structure was solved using the Bruker SHELXTL-PC[36] software by direct methods and refined by full-matrix least-squares methods on F^2. Hydrogen atoms were included in calculated positions and refined in the riding mode. For **4b·CH$_2$Cl$_2$** convergence was reached at a final $R1 = 0.0377$ [for $I > 2\sigma(I)$], $wR2 = 0.0789$ (for all data), 437 parameters, with allowance for the thermal anisotropy of all non-hydrogen atoms. The weighting scheme employed was $w = \{\sigma^2[F_o^2 + (0.0346P)^2]\}$, with $P = (|F_o|^2 + 2|F_c|^2)/3$ and the goodness of fit on F^2 was 0.923 for all observed reflections. For *fac*-**7b·(CH$_3$)$_2$CO** convergence was reached at a final $R1 = 0.0438$ [for $I > 2\sigma(I)$], $wR2 = 0.1221$ (for all data), 668 parameters, with allowance for the thermal anisotropy of all non-hydrogen atoms. The weighting scheme employed was $w = [\sigma^2(F_o)^2 + (0.0703P)^2 + (0.867P)]$, with $P = (|F_o|^2 + 2|F_c|^2)/3$ and the goodness of fit on F^2 was 1.080 for all observed reflections. CCDC-223473 (**4b·CH$_2$Cl$_2$**)

Table 3. Crystallographic data for **4b·CH$_2$Cl$_2$** and *fac*-**7a·(CH$_3$)$_2$CO**

	4b·CH$_2$Cl$_2$	*fac*-**7a·(CH$_3$)$_2$CO**
Empirical formula	$C_{36}H_{34}Cl_6N_2P_2Ru$	$C_{51}H_{51}B_2F_8N_6OP_3Ru$
Formula mass	870.36	1131.58
Temperature [K]	173(2)	296(2)
Wavelength [Å]	0.71073	0.71073
Crystal system	Monoclinic	Triclinic
Space group	$P2_1/n$	$P\bar{1}$
Unit cell dimensions	a = 15.756(3) Å	a = 12.296(3) Å
	b = 15.106(3) Å	b = 13.030(2) Å
	c = 15.771(3) Å	c = 18.068(4) Å
	α = 90°	α = 78.252(15)°
	β = 101.554(3)°	β = 88.132(18)°
	γ = 90°	γ = 67.028(17)°
Volume [Å^3]	3677.7(1)	2605.9(10)
Z	4	2
Density (calculated) [Mg/m^3]	1.572	1.442
Absorption coefficient [mm^{-1}]	0.979	0.465
F(000)	1760	1156
Crystal size [mm]	0.26 × 0.23 × 0.10	0.50 × 0.30 × 0.30
Index ranges	$-19 \le h \le 18$, $-18 \le k \le 15$, $-16 \le l \le 19$	$-15 \le h \le 16$, $-17 \le k \le 17$, $-23 \le l \le 23$
Reflections collected	22750	28912
Independent reflections	7606 [R(int) = 0.0712]	11344 [R(int) = 0.0300]
Data/restraints/parameters	7606/0/437	11344/0/668
Goodness-of-fit on F^2	0.923	1.080
Final R indices [$I > 2\sigma(I)$]	$R1$ = 0.0377, $wR2$ = 0.0715	$R1$ = 0.0438, $wR2$ = 0.1186
$\Delta\rho_{max/min}$ [e·Å^{-3}]	0.561/−0.709	0.843/−0.455

and -223474 [*fac*-**7b**·$(CH_3)_2CO$] contain the supplementary crystallographic data for this paper. These data can be obtained free of charge at www.ccdc.cam.ac.uk/conts/retrieving.html [or from the Cambridge Crystallographic Data Centre, 12 Union Road, Cambridge CB2 1EZ, UK; Fax: (internat.) + 44-1223-336-033; E-mail: deposit@ccdc.cam.ac.uk].

Acknowledgments

We are grateful to the Spanish DGES/MCyT (Project N. BQU-2002-00286) and Consejería de Ciencia y Tecnología de la Junta de Comunidades de Castilla-La Mancha (PBI-02-002) for financial support. We also thank to J. J. Delgado and A. M. Arnáiz from SCAI, University of Burgos, Spain for carrying out elemental analyses and FAB^+ mass spectra.

[1] [1a] T. Naota, H. Takaya, S.-I. Murahashi, *Chem. Rev.* **1998**, *98*, 2599−2660. [1b] P. A. Chaloner, M. A. Esteruelas, F. Joó, L. A. Oro, *Homogeneous Hydrogenation*, Kluwer, London, **1994**. [1c]R. A. Sánchez-Delgado, M. Rosales, *Coord. Chem. Rev.* **2000**, *196*, 249−280. [1d] K. Nomura, *J. Mol. Catal. A, Chem.* **1998**, *130*, 1−28.

[2] F. H. Jardine, *Prog. Inorg. Chem.* **1984**, *32*, 265 and references cited therein.

[3] [3a] A. M. Stolzenberg, E. L. Muetterties, *Organometallics* **1985**, *4*, 1739−1742. [3b] B. R. James, L. D. Markham, D. K. W. Wang, *J. Chem. Soc., Chem. Commun.* **1974**, 439.

[4] [4a] R. H. Fish, A. D. Thormodsen, G. A. Cremer, *J. Am. Chem. Soc.* **1982**, *104*, 5234−5237. [4b] R. H. Fish, J. L. Tan, A. D. Thormodsen, *Organometallics* **1985**, *4*, 1743−1747.

[5] G. P. Pez, R. A. Grey, J. Corsi, *J. Am. Chem. Soc.* **1981**, *103*, 7528−7535.

[6] [6a] Y. Sasson, P. Albin, J. Blum, *Tetrahedron Lett.* **1974**, 833−836. [6b] J. Tsuji, H. Suzuki, *Chem. Lett.* **1977**, 1085. [6c] R. A. Sánchez-Delgado, O. L. de Ochoa, *J. Mol. Cat.* **1979**, *6*, 303−305. [6d] R. A. Sánchez-Delgado, O. L. de Ochoa, *J. Organomet. Chem.* **1980**, *202*, 427−434. [6e] R. A. Sánchez-Delgado, A. Andriollo, O. L. de Ochoa, T. Suárez, N. Valencia, *J. Organomet. Chem.* **1981**, *209*, 77−83.

[7] B. R. James, L. D. Markham, *Inorg. Chem.* **1974**, *13*, 97−100.

[8] P. W. Armit, A. S. F. Boyd, T. A. Stephenson, *J. Chem. Soc., Dalton Trans.* **1975**, 1663.

[9] [9a] Y. Sasson, G. L. Rempel, *Tetrahedron Lett.* **1974**, 3221−3224. [9b] Y. Sasson, J. Blum, *J. Org. Chem.* **1975**, *40*, 1887−1896. [9c] Y. Sasson, G. L. Rempel, *Tetrahedron Lett.* **1974**, 4133−4136. [9d] M. Dedieu, Y. L. Pascal, *J. Mol. Catal.* **1980**, *9*, 71−90.

[10] M. A. Jalil, T. Yamada, S. Fujinami, T. Honjo, H. Nishikawa, *Polyhedron* **2001**, *20*, 627−633.

[11] For the ability of these precursors to form Ru^{II} derivatives bearing P,N-donor ligands see: [11a] A. Caballero, F. A. Jalón, B. R. Manzano, *Chem. Commun.* **1998**, 1879−1880. [11b] P. Braunstein, F. Naud, A. Pfaltz, S. J. Rettig, *Organometallics* **2000**, *19*, 2676−2683.

[12] [12a] G. R. Newkome, *Chem. Rev.* **1993**, *93*, 2067−2089. [12b] P. Espinet, K. Soulantika, *Coord. Chem. Rev.* **1999**, *193−195*, 499−556.

[13] P. E. Garrou, *Chem. Rev.* **1981**, *81*, 229−266.

[14] G. E. Rodgers, W. R. Cullen, B. R. James, *Can. J. Chem.* **1983**, 1314.

[15] M. S. Lupin, B. L. Shaw, *J. Chem. Soc., A* **1968**, 741.

[16] [16a] A. V. Marchenko, J. C. Huffman, P. Valerga, M. J. Tenorio, M. C. Puerta, K. G. Caulton, *Inorg. Chem.* **2001**, *40*, 6444−6450. [16b] J. S. Kingsbury, J. P. A. Harrity, P. J. Bonitatebus Jr., A. H. Hoveyda, *J. Am. Chem. Soc.* **1999**, *121*, 791−799. [16c] B. Deschamps, F. Mathey, J. Fischer, J. H. Nelson, *Inorg. Chem.* **1984**, *23*, 3455−3462. [16d] F. A. Cotton, M. Matusz, R. C. Torralba, *Inorg. Chem.* **1989**, *28*, 1516−1620.

[17] A. R. Chakravarty, F. A. Cotton, M. P. Diebold, D. B. Lewis, W. J. Roth, *J. Am. Chem. Soc.* **1986**, *108*, 971−1976.

[18] S. Pal, S. Pal, *Inorg. Chem.* **2001**, *40*, 4807−4810.

[19] For other examples with asymmetric chloride bridges, see refs.[11b,16c,18]

[20] J. S. Field, R. J. Haines, C. J. Parry, *J. Chem. Soc., Dalton Trans.* **1997**, 2843−2848.

[21] [21a] K. G. Caulton, *J. Am. Chem. Soc.* **1974**, *96*, 3005−3006. [21b] P. R. Hoffmann, K. G. Caulton, *J. Am. Chem. Soc.* **1975**, *97*, 4221−4228.

[22] [22a] T. A. Stephenson, G. Wilkinson, *J. Inorg. Nucl. Chem.* **1966**, *28*, 945. [22b] B. R. James, L. D. Markham, *Inorg. Chem.* **1974**, *13*, 97−100.

[23] P. W. Armit, A. S. F. Boyd, T. A. Stephenson, *J. Chem. Soc., Dalton Trans.* **1975**, 1663.

[24] A. von Zelewsky. *Stereochemistry of Coordination Compounds*, Wiley, Chichester, **1996**.

[25] [25a] C. G. Arena, E. Rotondo, F. Faraone, M. Lanfranchi, A. Tiripicchio, *Organometallics* **1991**, *19*, 3877−3885. [25b] D. Drommi, C. G. Arena, F. Nicoló, G. Bruno, F. Faraone, *J. Organomet. Chem.* **1995**, *485*, 115−121. [25c] R. E. Rülke, V. E. Kaasjager, P. Wehman, C. J. Elsevier, P. W. N. M. van Leeuwen, K. Vrieze, J. Fraanje, K. Goubitz, A. L. Spek, *Organometallics* **1996**, *15*, 3022−3031. [25d] B. Therrien, T. R. Ward, *Angew. Chem. Int. Ed.* **1999**, *38*, 405−408; Angew. Chem. **1999**, *111*, 418−421. [25e] P. Braunstein, M. D. Fryzuk, F. Naud, S. J. Rettig, *J. Chem. Soc., Dalton Trans.* **1999**, 589−594.

[26] K. Mashina, Y. Kaneda, A. Fukumoto, M. Tanaka, K. Tani, H. Nakano, A. Nakumura, *Inorg. Chim. Acta* **1998**, *270*, 459.

[27] M. A. Jalil, T. Yamada, S. Fujinami, T. Honjo, H. Nishikawa, *Polyhedron* **2001**, *20*, 627−633.

[28] [28a] B. K. Keppler, W. Rupp, U. M. Juhl, H. Endres, R. Niebl, W. Balzer, *Inorg. Chem.* **1987**, *26*, 4366−4370. [28b] M. Tadokoro, H. Kanno, T. Kitajima, H. Shimada-Umemoto, N. Nakanishi, K. Isobe, K. Nakasuji, *Proc. Nat. Acad. Sci. USA* **2002**, *99*, 4950−4955.

[29] B. Moreno, S. Sabo-Etienne, B. Chaudret, A. Rodríguez, F. Jalón, S. Trofimenko, *J. Am. Chem. Soc.* **1995**, *117*, 7441−7451.

[30] [30a] M. L. Christ, S. Sabo-Etienne, G. Chung, B. Chaudret, *Inorg. Chem.* **1994**, *33*, 5316−5319. [30b] L. S. MacFarlane, A. M. Joshi, S. J. Rettig, B. R. James, *Chem. Commun.* **1997**, 1363−1364.

[31] P. S. Hallman, T. A. Stephenson, G. Wilkinson, *Inorg. Synth.* **1970**, *12*, 237−240.

[32] [32a] A. C. Skapski, P. G. H. Troughton, *J. Chem. Soc., Chem. Commun.* **1968**, 1230−1231. [32b] R. A. Schunn, E. R. Wonchoba, *Inorg Synth.* **1972**, *13*, 131−134.

[33] M. Fajardo, A. de la Hoz, E. Diéz-Barra, F. A. Jalón, A. Otero, A. Rodríguez, J. Tejeda, D. Belletti, M. Lanfranchi, M. A. Pellinghelli, *J. Chem. Soc., Dalton Trans.* **1993**, 1935−1939.

[34] [34a] M. A. Bennett, T. N. Huang, T. W. Matheson, A. K. Smith, *Inorg. Synth.* **1982**, *21*, 74−75. [34b] M. A. Bennett, A. K. Smith, *J. Chem. Soc., Dalton Trans.* **1974**, 233−241.

[35] G. M. Sheldrick, *SADABS, Program for absorption corrections using Bruker CCD data*, University of Göttingen, Germany, **1996**.

[36] PC version, Bruker Analytical X-ray Systems, Madison, WI, **1995**.

Received December 2, 2003
Early View Article
Published Online April 7, 2004

